J Psychopharmacol OnlineFirst, published on April 22, 2010 as doi:10.1177/0269881110362126

Original Paper

Psychopharm

Journal of Psychopharmacology
0(00) 1–14

DOI: 10.1177/0269881110362126
jop.sagepub.com
SAGE

Differential effects produced by ketamine on oscillatory activity recorded in the rat hippocampus, dorsal striatum and nucleus accumbens

Mark J Hunt[1], Monika Falinska[1], Szymon Łęski[2], Daniel K Wójcik[2] and Stefan Kasicki[1]

Abstract

Previously, we showed that NMDA antagonists enhance high-frequency oscillations (130–180 Hz) in the nucleus accumbens. However, whether NMDA antagonists can enhance high-frequency oscillations in other brain regions remains unclear. Here, we used monopolar, bipolar and inverse current source density techniques to examine oscillatory activity in the hippocampus, a region known to generate spontaneous ripples (~200 Hz), its surrounding tissue, and the dorsal striatum, neuroanatomically related to the nucleus accumbens. In monopolar recordings, ketamine-induced increases in the power of high-frequency oscillations were detected in all structures, although the power was always substantially larger in the nucleus accumbens. In bipolar recordings, considered to remove common-mode input, high-frequency oscillations associated with ketamine injection were not present in the regions we investigated outside the nucleus accumbens. In line with this, inverse current source density showed the greatest changes in current to occur in the vicinity of the nucleus accumbens and a monopolar structure of the generator. We found little spatial localisation of ketamine high-frequency oscillations in other areas. In contrast, sharp-wave ripples, which were well localized to the hippocampus, occurred less frequently after ketamine. Notably, we also found ketamine produced small, but significant, changes in the power of 30–90 Hz gamma oscillations (an increase in the hippocampus and a decrease in the nucleus accumbens).

Keywords

hippocampus, ketamine, nucleus accumbens, schizophrenia, synchronization

Introduction

Oscillatory activity is believed to underlie information processing and encoding in the healthy brain (Singer, 1999). Several frequency bands recorded in local field potentials have been classically distinguished in neural systems, for example, delta (0–4 Hz), theta (6–12 Hz), gamma (30–90 Hz). In recent years, much faster high-frequency oscillations (HFO, >120 Hz, sometimes referred to as high-gamma) have been identified in vivo in several regions of the rat brain including the hippocampus (Buzsaki et al., 1983), basolateral amygdala (Ponomarenko et al., 2003), dorsal striatum (Masimore et al., 2004) and several regions of the cortex (Chrobak and Buzsaki, 1996; Jones and Barth, 1999). Fast oscillatory activity up to 200 Hz has also been found in the human brain (Canolty et al., 2006; Crone et al., 2006; Draguhn et al., 2000) and has also been identified in the human nucleus accumbens (NAc) (Cohen et al., 2009). The study of HFO in normal physiology and models of diseases is an emerging field of research. We have shown previously that HFO (130–180Hz) are enhanced by NMDA receptor antagonists in the NAc (Hunt et al., 2006), a brain region implicated in schizophrenia (Grace, 2000). These findings are of particular interest since subanaesthetic doses of NMDA receptor antagonists, such as ketamine are known to produce a transient schizophrenia-like state in humans, and in animals these compounds are used to model certain aspects of schizophrenia (Krystal et al., 1994; Lahti et al., 1995; Large et al., 2005; Sams-Dodd, 1999). Therefore, understanding the nature of abnormal oscillatory activity in the NMDA hypofunction model may shed light onto the underlying networks associated with psychosis.

In this study, we wanted to examine whether ketamine would enhance HFO in brain regions other than the NAc in freely moving rats. To address this issue, we chose the hippocampus, since it is structure known to be capable of generating fast oscillatory activity (ripples ~200 Hz) associated with sharp-waves (Buzsaki, 1986; Chrobak and Buzsaki, 1996). The hippocampus is a structure that coordinates memory formation and contextual processing, and abnormal functioning of this structure has been implicated in schizophrenia. For recent reviews see Boyer et al. (2007) and Freedman and Goldowitz (2009). Further, modulation of

[1]Laboratory of the Limbic System, Nencki Institute of Experimental Biology, Warsaw, Poland.
[2]Laboratory of Visual System, Nencki Institute of Experimental Biology, Warsaw, Poland.

Corresponding author:
Mark J Hunt, Laboratory of the Limbic System, Nencki Institute of Experimental Biology, 3 Pasteur Street, 02-093 Warsaw, Poland.
Email: mhunt@nencki.gov.pl

firing patterns of neurons in the NAc have been shown to be temporally associated with ripples recorded in the CA1 region (Pennartz et al., 2004) and we have shown previously that ketamine can modify synaptic efficacy in the hippocampus-NAc pathway (Hunt et al., 2005). We also examined whether ketamine would enhance oscillatory activity of high frequencies in the dorsal striatum, which is neuroanatomically related to the NAc. These structures both comprise predominantly of medium spiny GABAergic projection neurons and receive excitatory cortical projections (Wilson, 1993). Importantly, neurons of both structures share similar membrane potential features characterized by depolarized 'up' and hyperpolarized 'down' states (O'Donnell and Grace, 1995; Wilson and Kawaguchi, 1996).

Materials and methods

Experimental subjects

Experiments were performed on 25 male Wistar rats (250–350 g). In 11 rats, electrode pairs made from twisted tungsten wire (125 μm, Science Products, Germany), insulated except at the tip, were implanted in the dorsal CA1 region of the hippocampus (AP −3.8, ML 2.0, DV 2.2 mm) and the NAc (AP 1.6, ML 0.8, DV 7 mm) according to co-ordinates of the stereotaxic atlas (Paxinos and Watson, 1986). In a separate study four rats were implanted with electrodes in the dorsal striatum (AP −0.5, ML 3.5, DV 4 mm) and NAc. A silver wire was used as ground/reference electrode connected to a screw posterior to the bregma. The third test group of five male Wistar rats (accumbal group) were implanted with an array of six tungsten (70 μm) electrodes with each electrode tip separated by approximately 1 mm in the vertical plane to record both above and within the NAc. An additional five rats (hippocampal group) were implanted using an array of five electrodes to record across the dorsal hippocampus, with a sixth electrode implanted in the NAc. The location of the electrodes' tips was determined on 40 μm Cresyl violet stained sections. All necessary measures were taken to minimize pain or discomfort and the number of experimental animals used in this study. All experiments were conducted in accordance with the European community guidelines on the Care and Use of Laboratory Animals (86/609/EEC) and approved by a local ethics committee.

Experimental procedure

One week after surgery rats were handled and habituated to the recording chamber (44 cm × 50 cm × 42 cm). Local field potentials (LFPs) were recorded through a JFET preamplifier, amplified × 1000, filtered 1.0–1000 Hz (A-M Systems, USA), digitized at 8 kHz (Micro1401, CED, Cambridge, UK). Horizontal locomotor activity, assessed by photocell beam breaks (Columbus Instruments, USA), and LFPs were recorded simultaneously. Experiments were performed according to the Latin-square design, therefore each rat was injected twice in a pseudorandomized order with either ketamine 25 mg/kg (Sigma, Poland) or saline.

Power spectra. The digitized LFP signals were visually inspected and data segments with artefacts were removed manually and discarded for further analysis. Bipolar signals were generated by creating virtual channels calculated from the two symmetric monopolar signals. A similar method has been used previously to derive the bipolar signal (DeCoteau et al., 2007) and is believed to provide a more precise analysis of locally generated currents. Although most of the analysis was performed using the bipolar signal, occasionally we present monopolar signals. Mean power spectra of the LFP were carried out on successive 60-s data blocks using a fast Fourier transform of 4096 points. Where possible the average power of electrode pairs implanted in the NAc and CA1 region was calculated. Integrated power of delta (0–4 Hz), gamma (30–90 Hz) and HFO (130–180 Hz) was calculated.

Sharp-wave ripples. Bipolar LFPs in the hippocampal group were calculated by subtracting monopolar signals recorded from adjacent pairs of electrodes within or that straddled the CA1 region. The signals were digitally filtered 120–220 Hz (Finite Impulse Response filter) and the mean amplitude and standard deviation (SD) of the filtered signal calculated at baseline for each rat. Events corresponding to a peak, when the peak-to-peak amplitude exceeded 7 SD, were extracted from the filtered waveform. From the event signal we extracted bursts (at least two events with a peak-to-peak interval of a maximum of 10 ms).

Averaging. The start of the burst was used as a trigger to calculate the waveform average associated by the HFO. Averaged LFPs were obtained for the last 10-min baseline period (BL) and 0–10 min (KET 10) and 30–40 min (KET 40) after injection of ketamine.

Inverse current source density method. For hippocampal and accumbal groups, to localize the current sources generating recorded potentials we used the inverse current source density method (iCSD) (Leski et al., 2007; Pettersen et al., 2006; Wojcik and Leski, 2010). In this technique one assumes a specific form of the current source density (CSD) in the probed tissue (in our case, spline interpolated between the recording points) parameterized with as many parameters as the number of recordings. One then finds the relation between the potentials measured on the grid given the assumed CSD distribution and the parameters of the CSD. Inverting this relation one obtains the CSD in the tissue as a function of the measured potentials. This technique affords a better estimation of CSD from data than the traditional technique and gives a better control over the assumptions made (Leski et al., 2007; Pettersen et al., 2006). To calculate the CSD we used the code extracted from the CSD plotter tool created by Klas H Pettersen (Pettersen et al., 2006; see also http://software.incf.org/software/csdplotter/home).

Passive spread model. To generate reference data for some conjectures raised by the experiments we modelled the passive

spread of the electrical field from NAc to hippocampus. To approximate the dominating features of the observed structure of the field in NAc we assumed a single monopolar (spherical) source centred on the (AP 1.7, ML 1.5, DV 7.0 mm) and the amplitude of the source A(t) proportional to the signal recorded in NAc. We further assumed that the medium is purely resistive, isotropic and homogeneous. We calculated the LFP, which would be measured at five locations, $i = 1, \ldots, 5$, in the hippocampus and its vicinity (AP -3.25, ML 2.0, DV 1.8, 2.8, 3.8, 4.8 and 5.8 mm), if the rest of the brain was mute, using the inverse distance formula $V_i(t) = C\ A(t)\ /\ r_i$, where r_i was the distance between the source and the ith recording point (Nunez and Srinivasan, 2005), and C is a constant depending on resistivity of neural tissue and the assumed size of the source in NAc. We left this constant unspecified as we analysed only the relative strength of the signals recorded in the hippocampus. The calculated $V_i(t)$ were processed using the same iCSD technique as the hippocampal recordings.

Statistical analysis

Unless stated otherwise, data were analysed using repeated-measures ANOVA, followed by the Bonferroni *post hoc* test. Data are presented as mean ± SEM. Differences were considered statistically significant if $p \leq 0.05$.

Results

Local field potentials were recorded in the NAc, hippocampus and dorsal striatum. For each structure we used two monopolar recordings and the derived bipolar signal. This method for calculating the bipolar signal has been used previously (DeCoteau et al., 2007). We found no difference between the derived bipolar signal calculated off-line and the on-line bipolar signal (Supplementary Figure 1).

Analysis of oscillatory activity obtained using monopolar and bipolar recordings

Power spectra calculated for both mono- and bipolar signals recorded in the accumbens and hippocampus after injection of ketamine are shown in Figure 1A and B. HFO were visible in the bipolar signal from the NAc in all rats with electrodes correctly implanted in the NAc ($N = 7$). In contrast, in rats with implants in the CA1 region of the hippocampus HFO were absent in the bipolar signal despite being visible as a discrete peak in power spectra obtained from the monopolar signal ($N = 9$). Electrode placements are shown in Figure 1C and D. At the posterior border of the NAc HFO were weak in power spectra derived from the bipolar signal, despite being of substantial power in the monopolar signal after injection of ketamine (Figure 2A). A similar phenomenon was observed in the ventral lateral septal nucleus, where HFO were absent in the bipolar signal but of substantial power in the monopolar signal (Figure 2B).

In a separate group of rats ($N = 4$) local field potentials were recorded in the dorsal striatum. In all cases, the power of HFO after ketamine injection was extremely weak or absent in the bipolar signal, despite a marked increase in the power in both monopolar signals (Figure 2C). (Additional results from a depth profile analysis of the local field potentials recorded in the dorsal and ventral striatum are presented later in Figure 4).

Changes in oscillatory activity in bipolar signals recorded in the nucleus accumbens and hippocampus

Considering that bipolar recordings, by removing common-mode input, have been used to localize oscillatory activity to its generator (Brovelli et al., 2004; Brown et al., 2001; DeCoteau et al., 2007; Glasgow and Chapman, 2007; Magill et al., 2005), we subjected the bipolar signal in our studies to further analysis. The temporal dynamics of the integrated power of delta, gamma and HFO frequency bands are shown in Figure 3A–C. Individual time-courses showing changes in oscillatory activity for each frequency band are also shown from the electrodes correctly localized to the NAc ($N = 7$) and CA1 region of the hippocampus ($N = 9$). One-way repeated measures ANOVA revealed no significant effect for delta 0–4 Hz in the NAc or CA1 ($p > 0.05$, $F < 1.16$ for both). We found contrasting effects for the power of gamma 30–90 Hz, with significant decreases occurring in the NAc ($p = 0.0018$, $F = 1.665$), and increases in the CA1 region ($p < 0.0001$, $F = 2.785$). Consistent with our previous findings, after injection of ketamine the power of HFO 130–180 Hz rose significantly in the NAc ($p < 0.0001$, $F = 8.318$) and no effect was found in the CA1 region ($p > 0.05$, $F = 1.095$).

Depth-profile across the dorsal and ventral striatum

In an attempt to more precisely map the distribution of HFO across the dorsal and ventral striatum we performed depth profile analysis using six monopolar recordings simultaneously. Although we could not verify the precise recording location for all electrodes we found the deepest electrodes were localized to the NAc. Since the inter-electrode distance was known (approximately 1 mm) it was possible to estimate the electrode placement. In all cases, ketamine HFO were greatest in the deepest electrodes (Figure 4A). Notably, HFO were still detectable and appeared to be in phase even at the most distant electrode, several millimetres away. Typically, HFO were not observed in the bipolar signal derived using the three dorsal electrodes. We examined HFO in more detail using iCSD methodology, which permits more precise localization of the sources contributing to the oscillations (Figure 4B). As the electric potential is long-range, the measured LFPs present a blurred view of the underlying dynamics of the currents. Analysis of iCSD patterns indicated more localized enhancement of HFO in the NAc after ketamine injection. The mean magnitude of change calculated in the iCSD analysis across the electrode array is shown in Figure 4B ($N = 4$ rats). One rat was excluded from the analysis for technical reasons, but this rat also showed a similar pattern of change, with the greatest increase in current found at the deepest electrode. On the basis of our iCSD analysis, ketamine-enhanced HFO in the

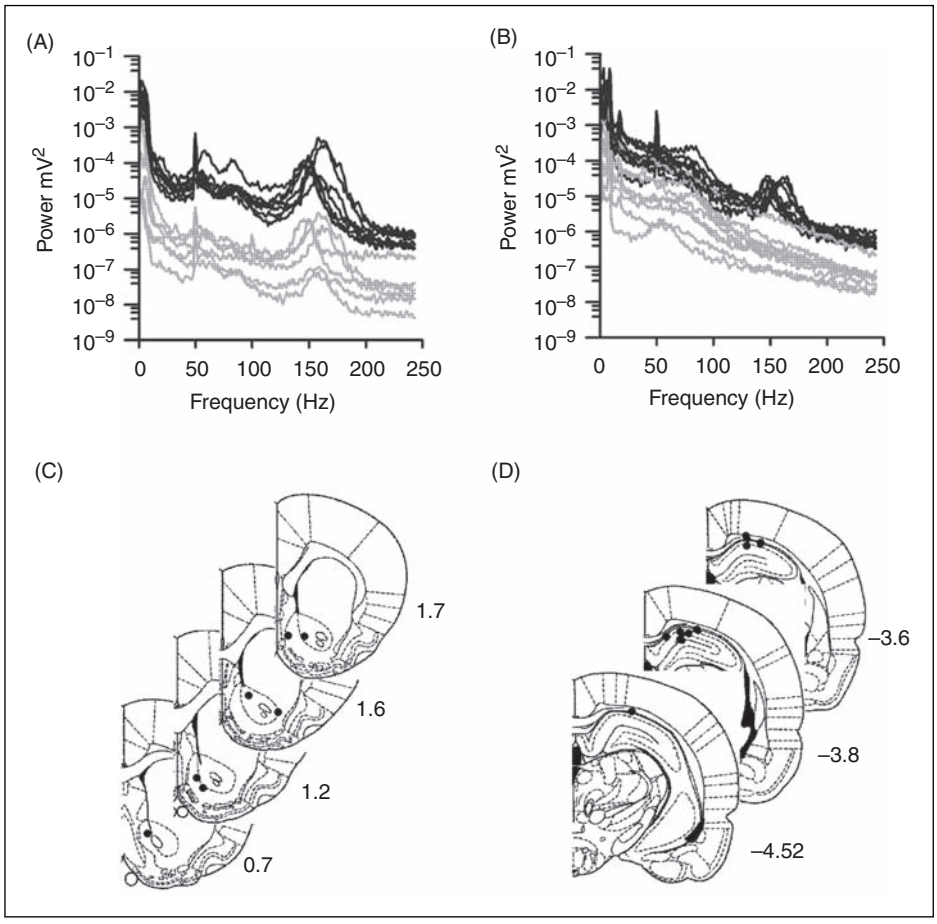

Figure 1. Power spectra calculated for monopolar (black) and derived bipolar (grey) LFP for the 60-s epoch around 5 min after injection of 25 mg/kg ketamine. Data are shown for individual rats with electrodes in the NAc and CA1 region of the hippocampus (A, B). The power of oscillatory activity recorded in the local field potentials of bipolar recordings was substantially smaller than those recorded in the monopolar field potential. Notably, HFO were present in mono- and bipolar activity of NAc, while in hippocampus HFO were present only in the monopolar signal. Y-axes are expressed using the $\log_{10}$ scale. Electrode placements are shown for the NAc and hippocampus (C, D).

NAc seem to have a monopole structure which decays over distances like $1/r$. Assuming such relation we compared the plot of theoretical amplitude attenuation across the distance from the source with the plot of experimental data (Supplementary Figure 2) and found they fit well. Moreover, subtracting signals more distant from the site of the generator results in a much smaller difference of amplitude compared with the vicinity of the generator.

Depth profile across the hippocampus and surrounding structures

It may be argued that the bipolar arrangement may remove in-phase oscillatory activity of equivalent amplitude generated simultaneously at both electrode tips (Berke et al., 2004). This may particularly influence the symmetrical signal recorded in layered structures, such as the hippocampus. We therefore examined oscillatory activity using a five-electrode array which was designed to straddle the dorsal hippocampus (and its surrounding structures) and one electrode simultaneously recording from the NAc. Typically the shallowest electrode was located in the parietal association cortex and the deepest in the posterior thalamus. Middle electrodes were usually localized to the dorsal CA1, CA3 or dentate gyrus. Large amplitude spontaneous HFO, termed 'ripples', are an electrophysiological characteristic of hippocampal recordings (Buzsaki et al., 1983; Chrobak and Buzsaki, 1996; Csicsvari et al., 1998). In the band-pass filtered monopolar recordings, we found ripples visible from electrodes in the vicinity of the CA1 region of the hippocampus (Figure 5A, Baseline). Ripples were preserved in the bipolar signal of adjacent recordings. In line with the findings of others, ripples were approximately 180–200 Hz and typically associated with a large amplitude negative going wave (see Figure 7 below). In the presence of ketamine, smaller amplitude and lower frequency HFO (~150 Hz) were visible in the band pass filtered signal which appeared coherent across all electrodes and in phase with HFO recorded from the NAc (Figure 5A, ketamine, and Supplementary Figure 3).

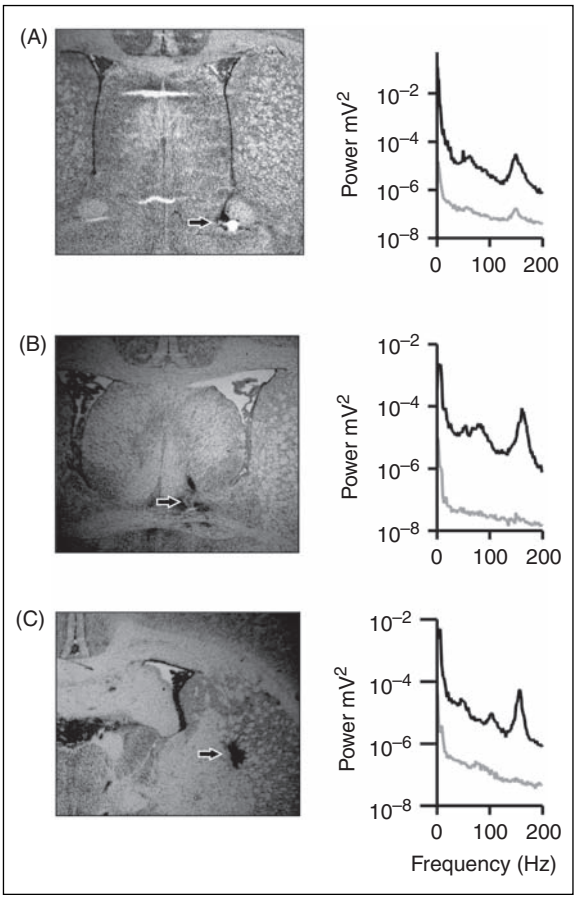

Figure 2. Power spectra for a 60-s interval after injection of ketamine are shown for electrodes located in posterior edge of the NAc (A), ventral lateral septal nucleus (B) and dorsal striatum (C). Power spectra for one of the monopolar signals are shown in black and the derived bipolar signal shown in grey. A prominent peak ~150 Hz was visible in the monopolar but not the bipolar signal. Y-axes are expressed using the $\log_{10}$ scale. Arrows indicate location of the recording site.

The phase coherence, and the coincidence of the lower frequency HFO in the hippocampus and in the NAc, is compatible with passive spread of the electrical potential from a single source in the NAc. Consistent with our findings using twisted electrode pairs, HFO were visible as a discrete peak in the power spectra calculated from all monopolar signals, but there was no comparable peak when using the bipolar signal (calculated from adjacent electrode pairs); see Figure 5B.

The iCSD analysis revealed that spontaneous HFO showed spatial localization to the CA1 region of the hippocampus and clear multipole structure with a stronger source in the middle and two weaker counterparts above and below (Figure 6A). In contrast, the HFO associated with injection of ketamine did not reveal any clear regional organization and iCSD analysis revealed a pattern of alternating stripes resembling a common artefact arising in analysis of passively propagated signals from a distant source. To verify the conjecture of accumbal origin and passive propagation of these oscillations we simulated this situation. Thus we assumed the only field source located in the NAc and the time-course of this source proportional to the simultaneously measured potential in NAc and we took into account the relative geometry of the studied structures (see the Methods section). On this basis we calculated the LFP which would be recorded in the hippocampal array. The 135–165 Hz band-pass was used since we wanted to limit the digitally filtered signal to the frequency range where ketamine-enhanced HFO are known to occur. Comparison of the iCSD profiles obtained from the filtered hippocampal recordings with the results of analysis of the model signals are shown in Figure 6B. We found a similar pattern of alternating stripes in both the experimental and model data associated with the occurrence of HFO in the NAc. The patterns we found in our analysis here are the artefact of the method used combined with the linear geometry of the electrode setup. This has led us to think that the most probable interpretation of the dominating part of the experimental data in the top panel of Figure 6B is a similar effect of passively propagated field from the NAc. Since the model data were generated from a single source located in the NAc, this result indicates that there are no sources or sinks to be found in the hippocampus concerning HFO after ketamine. The observed deviations between the experimental and model data may arise from the non-laminar structure of the studied part of the brain and in consequence non-homogeneity of the conductivity, and the fields generated in the neglected sources of the rest of the brain. Small deviations of the electrode positions from the assumed grid are probably less important.

Subanaesthetic dose of ketamine reduces the occurrence but not amplitude or frequency of spontaneous sharp-wave ripples

We went on to examine the impact of ketamine injection on spontaneous HFO. This was achieved using the bipolar signal, derived from adjacent electrodes, which, as shown in Figure 5, removes the majority of ketamine-associated HFO from the waveform. Spontaneous HFO were extracted at 7 SD baseline, which were large amplitude oscillatory events only. One-way ANOVA repeated measures revealed a significant effect of ketamine injection on ripple occurrence ($F = 10.00$, $p = 0.0067$; Figure 7). Bonferroni *post hoc* test revealed a reduction in the occurrence of ripples at baseline compared with the first 10 min after injection of ketamine (KET 10) ($p < 0.05$) but no significant difference at the 30–40 min post injection (KET 40) time point. There was also a significant difference between KET 10 and KET 40 time points ($p < 0.01$). However, the frequency (calculated by inter-event interval) and amplitude ($F = 2.745$, $p = 0.1237$) of ripples did not change over time. Ketamine produced a significant increase in locomotor activity (repeated measures, one-way ANOVA: $F = 64.90$, $p < 0.0001$, Bonferroni *post hoc*, BL versus KET 10 and KET 10 versus KET 40: both $p < 0.0001$). Considering that ripples are typically associated with quiet waking and slow-wave sleep and rarely occur during motor activity (Buzsaki, 1986; Buzsaki et al., 1983), it seems reasonable to assume that the increased locomotor activity immediately

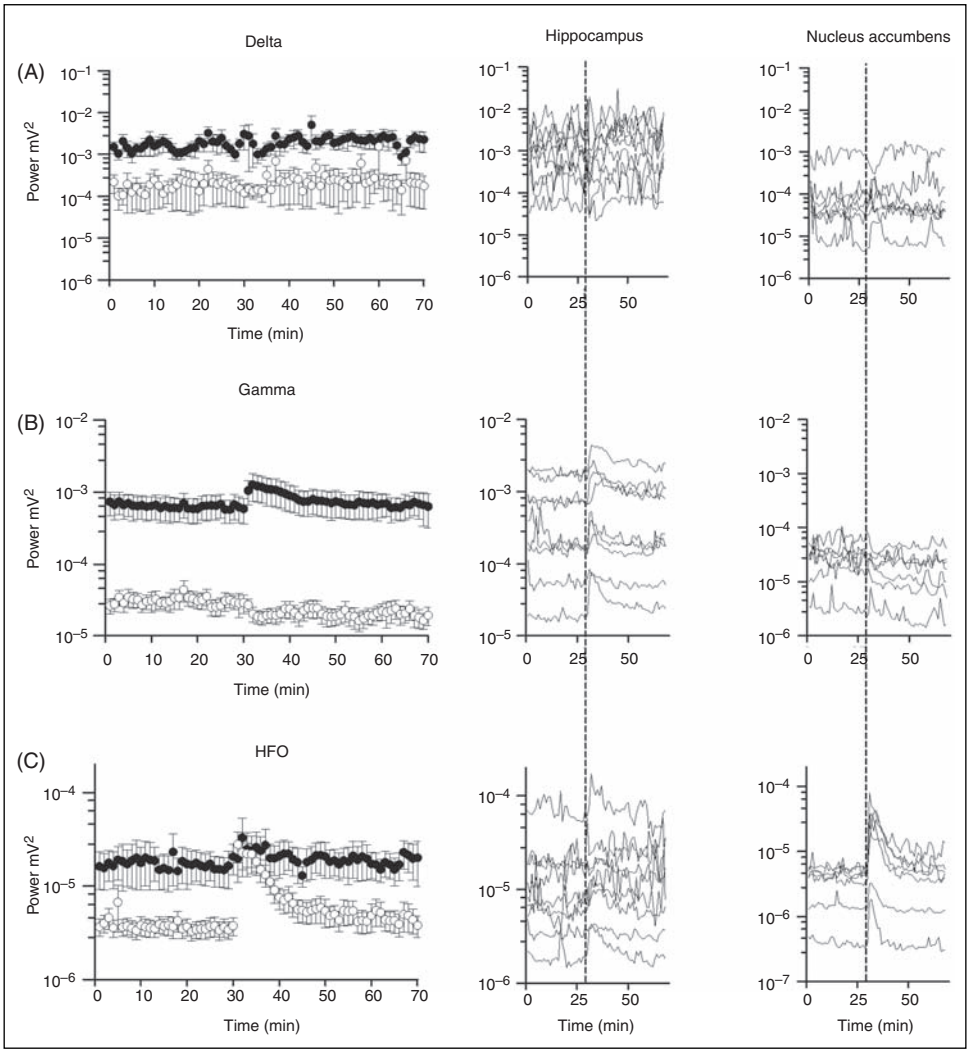

Figure 3. Time-courses showing the effect of intraperitoneal injection of ketamine 25 mg/kg on the averaged integrated power of delta (0–4 Hz), gamma (30–90 Hz) and HFO (130–180 Hz) frequency bands for the CA1 region (filled circles) of the hippocampus and NAc (non-filled circles) are presented in the left column (A–C). Individual time-courses for each rat are shown on the right side (individual points are power spectra calculated for 60-s epochs). The dashed vertical lines show the time of injection. Y-axes for the time-course graphs are expressed using the $\log_{10}$ scale.

after injection of ketamine (KET 10) most likely underlies the reduction in ripple occurrence. The duration ($F = 0.2735$, $p = 0.7676$) was not significantly different. At baseline, the waveform average for both the bipolar signal and the monopolar signal recorded in the radiatum of CA1 showed the occurrence of spontaneous hippocampal HFO was associated with a negative-going sharp-wave in 5/5 rats, which suggests the type of activity we record in this region is the same as that previously published by others. Examples of waveforms are shown in Figure 7B. Post injection of ketamine spontaneous HFO remained associated with a sharp wave in 4/5 rats. In one case the waveform average at KET 10 was not associated with a sharp-wave, but this is probably due to the low occurrence of HFO in this rat ($N = 4$ ripple events), rather than a direct effect of ketamine on this activity. We also examined the effect of a lower dose of ketamine (5 mg/kg) on ripple activity in four rats. One-way ANOVA repeated measures revealed that this dose did not substantially influence motor activity ($F = 2.022$, $p = 0.213$) and was not associated with any significant effect on ripple occurrence ($F = 0.1976$, $p = 0.8258$), amplitude ($F = 0.8994$, $p = 0.4554$), duration ($F = 0.03189$, $p = 0.9688$) or frequency ($F = 1.526$, $p = 0.2912$). Notably, ketamine anaesthesia has been shown to reduce the frequency, but did not prevent the generation, of ripples (Ylinen et al., 1995).

Discussion

Methodological considerations

In this study, we have examined changes in oscillatory activity occurring post injection of ketamine using monopolar local field potential recordings and their derived bipolar

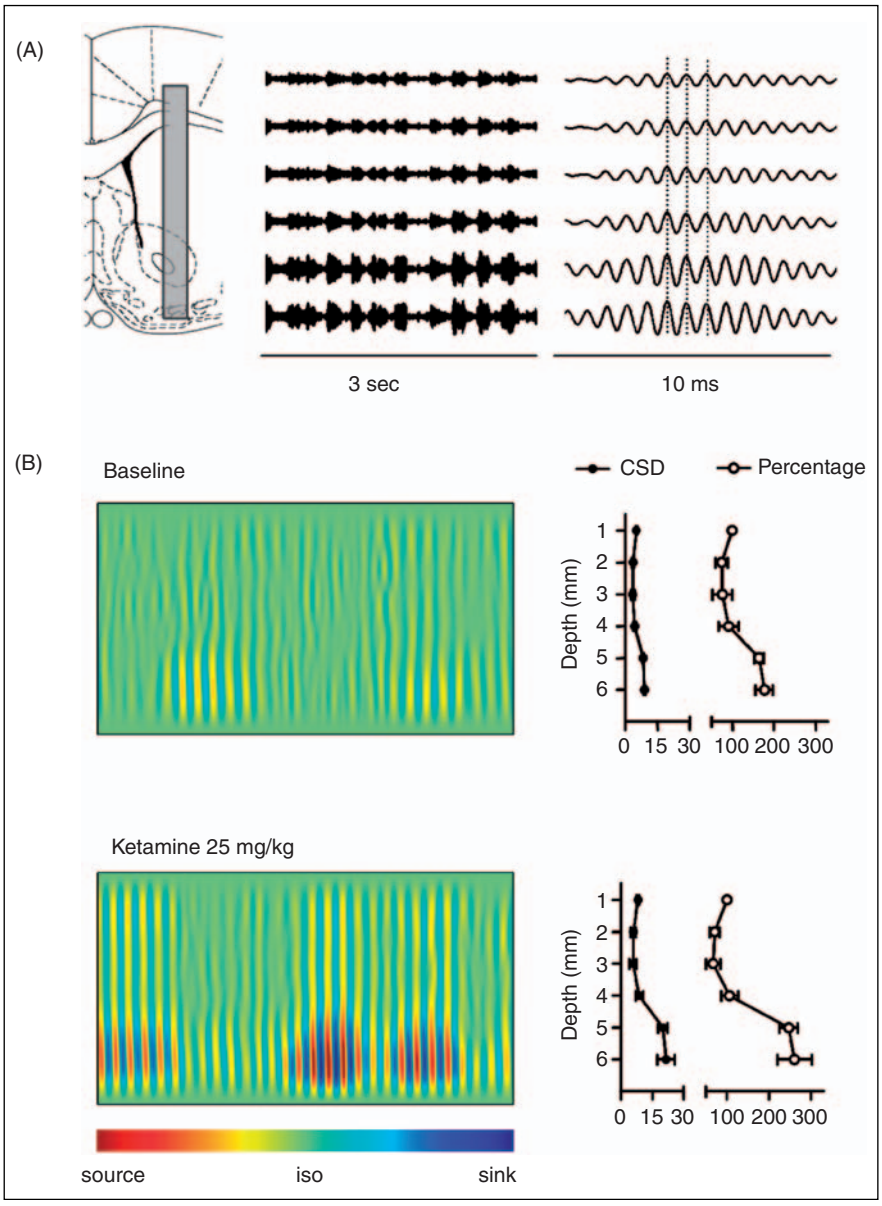

Figure 4. (A) Band-pass filtered 120–220 Hz field potentials, recorded simultaneously after injection of ketamine. Bursts of HFO are visible in the filtered signal in all channels; however, the amplitude is largest within the NAc. An example of a single burst of HFO is shown; note the oscillatory activity appears in-phase across all channels. (B) iCSD from the dorsal and ventral striatum. Example of iCSD at baseline and after injection of 25 mg/kg ketamine (both 3-s data segments). Horizontal axis is time, vertical is depth. The intensity in both plots is the same. Note that the structure of the field indicates alternating monopolar source in the accumbens. Observe the increased amplitude of oscillations after ketamine injection. Depth profile showing the mean and SEM ($N = 4$ rats) of the magnitude of CSD oscillations (rms) at baseline and after ketamine injection in the right-hand column.

counterpart calculated off-line by subtracting two monopolar recordings. Bipolar local field potentials are considered to remove common-mode input which may otherwise contaminate the signal. As such, the symmetrical signal provides a more reliable measure of local changes in oscillatory activity and is widely used to localize neural activity to its generator (Brovelli et al., 2004; Brown et al., 2001; Darbin et al., 2006; Finnerty and Jefferys, 2000; Glasgow and Chapman, 2007; Magill et al., 2005; Rajagovindan and Ding, 2008). Deriving the bipolar signal from two monopolar recordings has been used previously (DeCoteau et al., 2007; Fogelson et al., 2006; Sauleau et al., 2009) and in our study we found no difference between the symmetrical signal recorded on-line and derived bipolar signal calculated off-line. Also hippocampal ripples, which are known to be generated within the CA1 region, were clearly visible in both the monopolar and derived bipolar signal, which supports the use of a derived bipolar signal to localize the generator of oscillatory activity. Since we wanted to compare activity recorded in both the mono- and bipolar field potentials we chose this methodology.

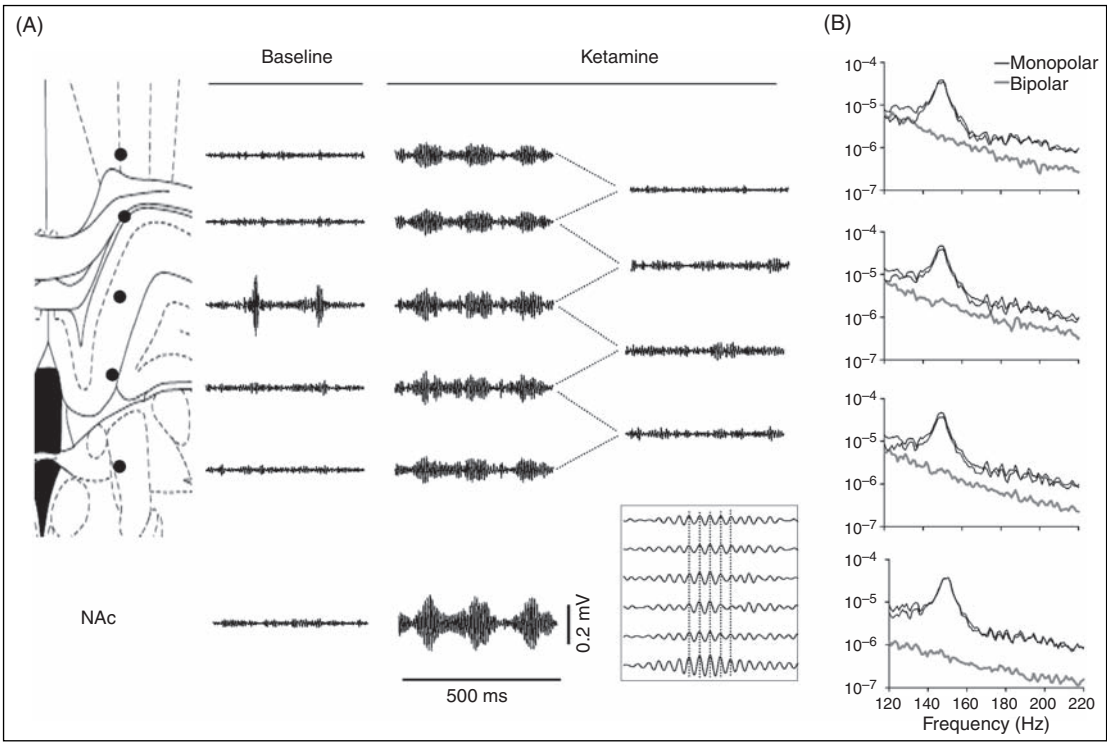

Figure 5. Depth profile of oscillatory activity recorded simultaneously across the hippocampus and neighbouring structures. (A) 120–220 Hz band-pass filtered local field potentials are shown for activity recorded at each electrode tip at baseline and after injection of ketamine 25 mg/kg. Spontaneous HFO bursts recorded at baseline were visible in the vicinity of the CA1 layer. In the presence of ketamine bursts of HFO of comparable amplitude were present across all electrodes in the array. Note that the bursts of HFO were closely associated and occurred in phase with bursts of HFO recorded in the NAc. Moreover, HFO were in phase for all channels (inset). Bursts of HFO in the hippocampal array were not preserved in the bipolar signals derived by subtracting adjacent monopolar recordings. (B) Power spectra for both monopolar field potentials (black) and the derived bipolar signal (grey). A discrete peak occurring around 150 Hz was visible in each of the monopolar recordings; however, this was not present in the bipolar signal.

The nucleus accumbens as a dominant source of high-frequency oscillations in striatal tissue

Consistent with our previous findings, we found that ketamine-enhanced HFO were substantial in monopolar recording from the NAc (Hunt et al., 2006) and were also detectable in bipolar recordings. In contrast, in the neuroanatomically-related dorsal striatum, ketamine-enhanced HFO were present in the monopolar signals (although of smaller amplitude) but not detectable in the power spectra from bipolar signals. We investigated this activity further using local field potentials recorded simultaneously in an array across the dorsal and ventral portions of the striatum. The amplitude of ketamine-enhanced HFO was substantially larger in electrodes located in the vicinity of the NAc. A 'shadow' of this activity could be recorded in-phase with NAc activity in electrodes implanted more dorsally, indicating the dominant changes occur in the NAc. HFO were substantially weaker in bipolar signals close to the posterior edge of the NAc and virtually absent in bipolar dorsal striatal recordings. Our findings suggest that the NAc is an important generator of HFO post injection of ketamine. In line with this, iCSD analysis revealed the strongest changes in current to be present in the vicinity of the NAc, both at baseline and post ketamine. Although striatal neurons can participate in the generation of large scale oscillatory activity as has been shown for lower frequencies (Berke et al., 2004), this does not appear to be the case for ketamine-enhanced HFO, which showed a much more localized activity to ventral portions.

Local injection of NMDA antagonist to the NAc is sufficient to enhance HFO comparable to values after systemic injection, indicating NAc circuitry is highly sensitive to NMDA blockade (Hunt et al., 2010). The substantial increase in the amplitude of HFO (typically 10-fold compared with baseline) occurring in the NAc probably reflects the generation of HFO by more numerous or larger clusters of accumbal neurons. Thus, the electric field generated by these clusters may be sufficient to be detected at distant recording sites. Indeed, ketamine-enhanced HFO in the NAc seem to have a monopole structure which decays over distances like $1/r$, which fitted the pattern of attenuation of HFO with distance. We consider that another remote synchronized monopole is unlikely and we speculate that the balance is provided by diffuse passive currents in larger volumes of the tissue surrounding the NAc.

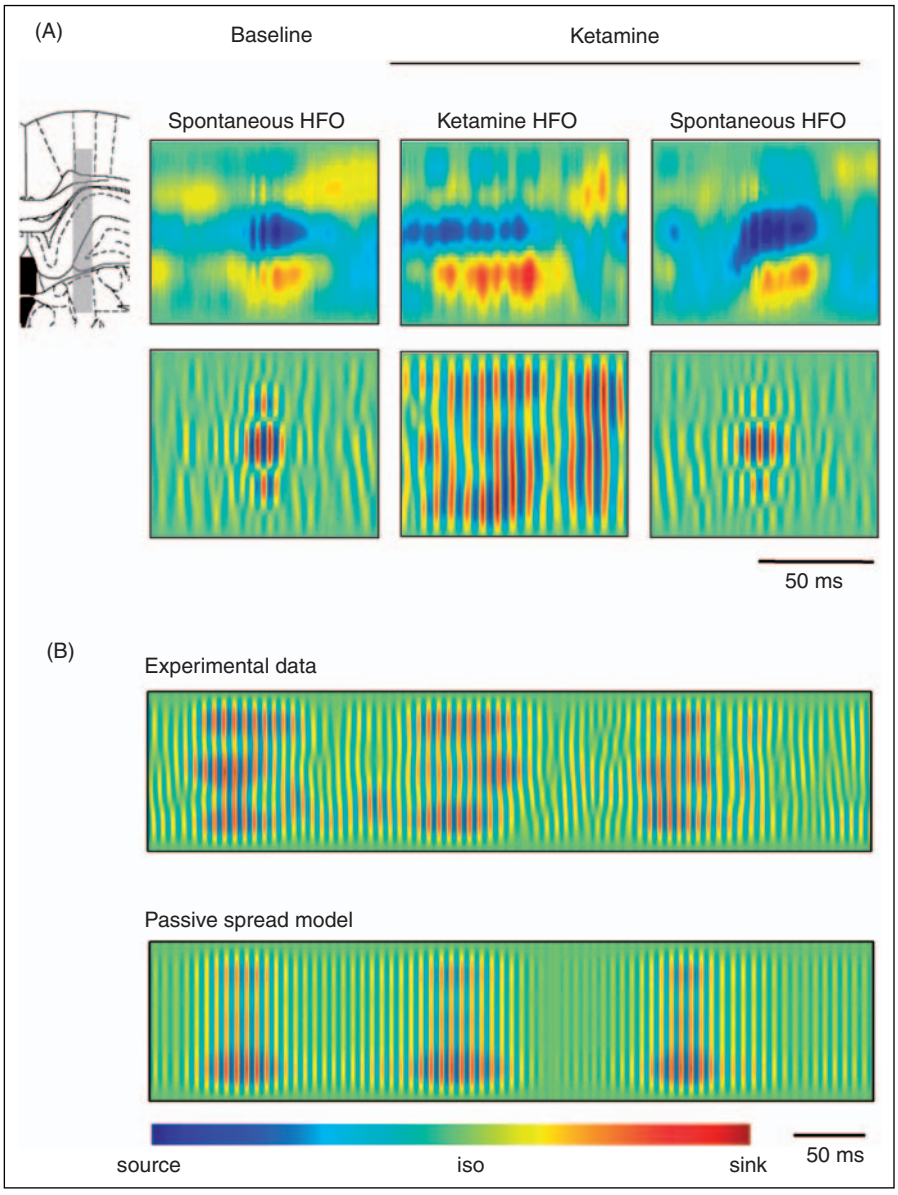

Figure 6. (A) iCSD from the hippocampus and surrounding tissue calculated for the raw signal (top panel) and the band-pass filtered 120–220 Hz signal (bottom panel). An example of spontaneous HFO recorded in the hippocampus at baseline associated with localized changes in current and a clear multipole structure with a stronger source in the middle and two weaker counterparts above and below. In contrast, there was a lack of discernible spatial localization for the ketamine-associated HFO, which appear equivalent across all electrodes. We also show an example of spontaneous HFO which were still visible in the presence of ketamine. Note, the dominant source and sink in the raw signal temporally associated with the occurrence of spontaneous HFO both at baseline and after ketamine. (B) 500-ms data segment showing iCSD across the hippocampal array from the experimental data (135–165 Hz) and passive conduction model which predicts the pattern of conduction of HFO from the NAc. We assume that the deviations between the model and the experimental data are largely due to non-homogeneity of the conductivity, neglected sources other than NAc, or small deviations of the electrode positions from the assumed grid.

Dissociation between ketamine-high-frequency oscillations and sharp-wave ripples in the hippocampus

In the depth profile analysis across the hippocampus and surrounding tissues, spontaneous sharp-wave ripples, reminiscent of those described by Buzsaki and colleagues (Buzsaki et al., 1983; Chrobak and Buzsaki, 1996; Csicsvari et al., 1998; Ylinen et al., 1995) were substantial in the monopolar signal recorded from electrodes in the CA1 vicinity and were also preserved with a good signal-to-noise ratio in the bipolar signal. Consistent with the findings of others, ripples occurred at around 200 Hz, notably higher than ketamine-enhanced HFO. iCSD analysis revealed a clear spatial localization for spontaneously occurring hippocampal ripples which were

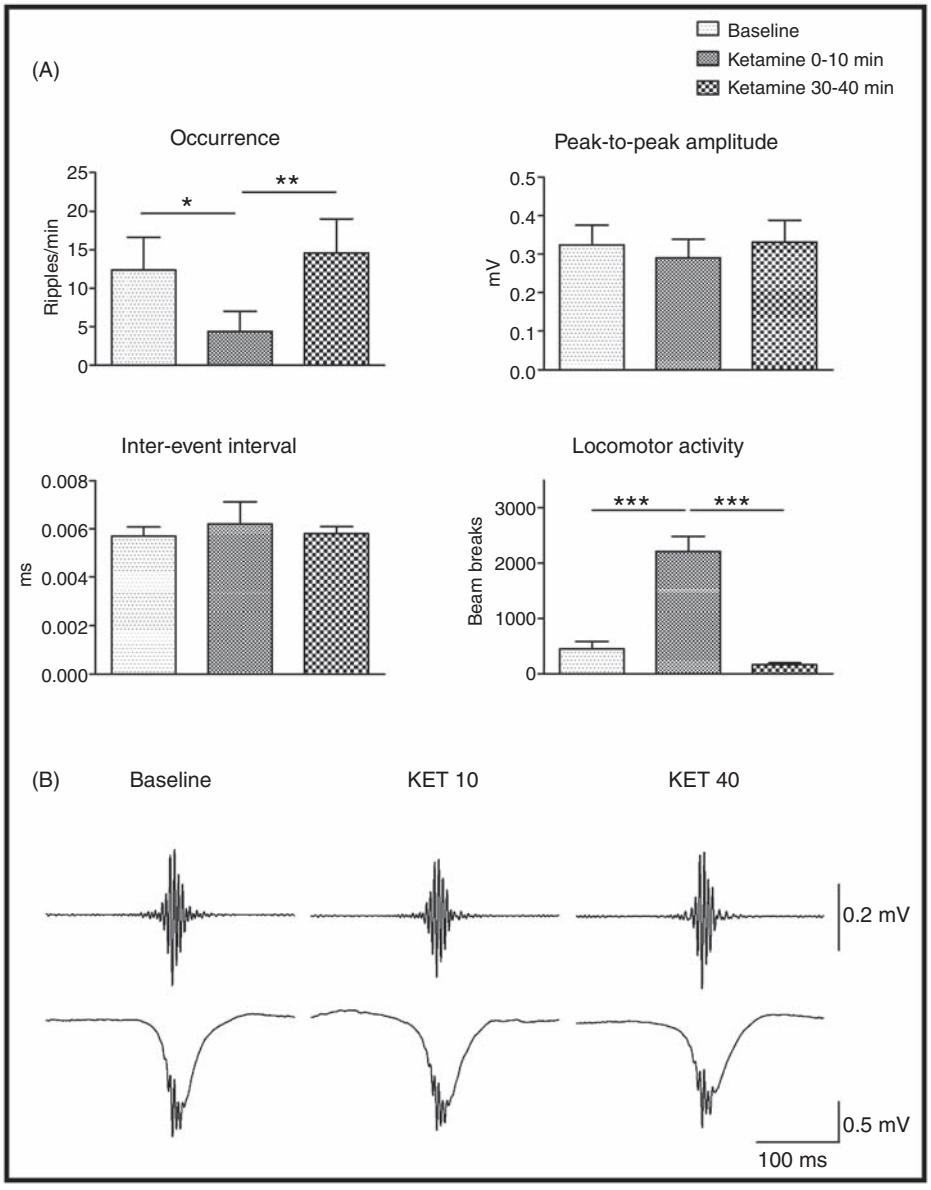

Figure 7. (A) The effect of ketamine on spontaneous sharp-wave ripples in the hippocampus. The mean occurrence, amplitude, frequency and locomotor activity are shown 10 min prior to injection at baseline, 0–10 min (KET 10) and 30–40 min (KET 40) after injection of ketamine 25 mg/kg. (B) Waveform averages of the band-pass filtered (120–220 Hz) signal and raw field potential (KET 10) triggered on the occurrence of ripples are also shown for each time-point. $*p < 0.05$; $**p < 0.01$; $***p < 0.001$.

associated with a dipole reversal about the CA1 layer (Ylinen et al., 1995). Injection of a subanaesthetic dose of ketamine, which provoked increased locomotor activity, was associated with a substantial reduction in the number of sharp-wave ripples. However, ketamine did not significantly change the intrinsic ripple characteristics (frequency, amplitude and duration), as was shown after an anaesthetic dose (Ylinen et al., 1995). Since ripples are generally associated with inactivity periods such as quiet waking and slow-wave sleep (Buzsaki et al., 1983), the reduced number may result from ketamine-induced hyperactivity. In line with this, systemic injection of a much lower dose of ketamine (5 mg/kg), which produced negligible motor excitation, did not modify the occurrence of spontaneous sharp-wave ripples.

Sharp-wave ripples appear to be involved in cognitive function (Buzsaki et al., 1990; Chrobak et al., 2000), and a reduction in ripple number, during slow-wave sleep, can lead to impaired spatial memory (Girardeau et al., 2009). Considering ketamine produces complex effects on cognitive performance in humans and animals

(Enomoto and Floresco, 2009; Krystal et al., 1994; Moghaddam et al., 1997; Verma and Moghaddam, 1996), it remains possible that the reduction in ripples observed after ketamine may impair higher cognitive function, rather than an epiphenomenon occurring as a consequence of behavioural activation. Further studies are warranted to determine whether chronic administration of ketamine, which impairs cognitive function, is associated with a reduction in ripple number.

In contrast to sharp-wave ripples, HFO after injection of ketamine were visible in all monopolar electrodes, of equivalent amplitude and in-phase across the array. Consistent with our findings from twisted electrodes, HFO were not detectable in any of the bipolar derivations. It may be argued that the bipolar arrangement removes in-phase oscillatory activity of equivalent amplitude generated simultaneously at both electrode tips (Berke, 2006). This may have a more prominent influence in layered structures, such as the hippocampus, if the electrode tips were on the same side of the generating dipole. However, this scenario is unlikely since HFO were absent in bipolar recordings independently of whether the electrodes were within or straddling the CA1 layer. Additionally, structural differences do not satisfactorily explain why HFO are not present in these bipolar recordings, since if it were merely an artefact of a layered structure, one should also expect HFO to be present in bipolar recordings from the dorsal striatum, as well as other non-laminar structures which was not the case in our study. In line with findings from field potential recordings, iCSD analysis did not show any clear spatial localization for ketamine-enhanced HFO, which appeared as almost uniformly alternating current sources and sinks across the electrode array and may represent a passively propagated signal from a distant source. Together, these findings support the notion that ketamine-enhanced HFO, unlike sharp-wave ripples, were not generated in the vicinity of the hippocampus.

Ketamine-enhanced high-frequency oscillation spread or synchronicity

The site of generation of ketamine-enhanced HFO in regions outside the NAc (dorsal striatum, hippocampus and its neighbouring structures – the parietal cortex and posterior thalamus, and in misplaced electrodes such as in the medial septum) is unclear. One possibility that should be considered is that ketamine-enhanced HFO detected at the recording tips, or by the low-impedance reference skull screw, may result from spread by volume conducted currents. Indeed, monopolar recordings but not bipolar recordings are likely to be influenced by shifts in the reference potential, which in our case was located close to the cortex (Darbin et al., 2006). The NAc appears to be a source of HFO, but it is possible that it is part of a much larger generator of ketamine-enhanced HFO, involving other limbic structures. For the present, spread of an electric field, involving the NAc, is the most parsimonious interpretation of our results (i.e. smaller amplitude, in-phase, removed by bipolar recordings and consistent with the passive field conduction model). This is not the case for the whole field, but only for the specific HFO band, possibly related to the substantial increase in this band after injection of ketamine. In cases where locally generated oscillatory activity of a given frequency band is absent or weak (which is typical for >100 Hz activity) far field activity may become more easily detected, since there is no interference with local activity. Although little is known about the spread of HFO, gamma oscillations (>40 Hz) can be detected a substantial distance from its point of origin, most notably in EEG scalp recordings. Also, within the striatum, it is likely that a proportion of the gamma oscillations is not generated locally, but may result from conduction from the underlying piriform cortex (Berke, 2006).

An alternative interpretation is that ketamine induces multiple sites of locally generated synchronous HFO. Whilst, from the perspective of monopolar recordings, this interpretation would explain the coherence between HFO in the NAc and other structures, it is hard to reconcile this with our other findings, such as differences in amplitude and absence of HFO in bipolar recordings. Further, long distance synchrony, which can occur in the brain, is typically associated with regions that have reciprocal communication or common input. The hippocampus projects directly to the NAc (Kelley and Domesick, 1982); however, there is no direct bidirectional interaction. Also, to our knowledge, there is no evidence that the other structures we examined, which also displayed in-phase HFO, directly receive or send projections to the NAc. Consequently, it would be hard to envisage a system of widely dispersed and synchronous HFO between non-directly communicating regions. It is also unlikely that the generation of ketamine-enhanced HFO is a general feature of NMDA receptor blockade, since one might expect ketamine to generate larger amplitude HFO in the hippocampus, as the density of receptors is greatest there. It thus appears that the ketamine-enhanced HFO in the regions we recorded outside the NAc are more likely 'synchrony' due to passive conduction, rather than 'true' synchrony induced dynamically.

Since ketamine increases locomotor activity it raises the possibility that muscle artefacts may contaminate the monopolar signal we recorded (muscle artefacts are typically removed in the bipolar signal; see Darbin et al., 2006). However, this is unlikely, since muscle artefacts would be expected to be of comparable amplitude in all channels, which was not the case for HFO recorded in our study. Also, ketamine-enhanced HFO were discernible as a discrete peak in the power spectra, which does not occur during movement artefacts, which typically produce a gradient with the power attenuating with frequency, or a random pattern in several high-frequency bands (Figure 5).

Enhanced high-frequency oscillations in the nucleus accumbens and the NMDA hypofunction model of schizophrenia

The membrane potential of most medium spiny neurons of the NAc may switch between two states – a hyperpolarized (down) or a ready-to-fire (up) – chiefly driven by hippocampal input (O'Donnell and Grace, 1995). However, trains of pulses applied to the prefrontal cortex (PFC) alone can also induce sustained depolarization of NAc neurons (Gruber and O'Donnell, 2009). Administration of MK801 to freely

moving rats increased the number of randomly distributed single spikes in most of the PFC projection neurons and also reduced burst firing of some PFC neurons (Homayoun and Moghaddam, 2007; Jackson et al., 2004). Since the PFC projects to the NAc, altered excitatory output of cortical neurons would be expected to produce measurable membrane potential changes of accumbal neurons, which may be reflected in the local field potential we record. It may be supposed, therefore, that the presence of enhanced HFO is related to perturbed membrane potential transitions. Indeed, membrane potential changes of accumbal neurons, attributed to altered hippocampal gating, have been reported in NAc neurons after administration of the NMDA receptor antagonist phencyclidine (PCP) (O'Donnell and Grace, 1998). Although these studies were conducted in anaesthetized rats, we have shown that ketamine, at a dose that enhances HFO, reduced hippocampal input to the NAc (Hunt et al., 2005). Considering that the awake state is critical for detecting HFO after ketamine (Hunt et al., 2009b), it is possible that reduced hippocampal input, combined with modified firing of PFC neurons leads to the generation of HFO in the NAc. In support of this, we have shown that lamotrigine, which can modify neuronal firing and is used as adjuvant treatment for schizophrenia (Large et al., 2005), reduced the power and frequency of ketamine-enhanced HFO (Hunt et al., 2008). Further studies using antipsychotic compounds such as clozapine, which can reverse the effect of MK801 on cortical neuronal firing (Homayoun and Moghaddam, 2007), as well as typical antipsychotic compounds are warranted to determine the validity of enhanced HFO in NMDA hypofunction models of schizophrenia.

Ketamine differentially modulates gamma activity in the hippocampus and the nucleus accumbens

Examination of other frequency bands showed a significant increase in the power of hippocampal gamma associated with injection of ketamine. This result is in line with previous studies using PCP (Ma and Leung, 2000, 2007). Increases in the power of gamma have also been observed in the neocortex of awake rats injected with ketamine or MK-801 (Hakami et al., 2009; Pinault, 2008). Recently, a cortical modelling study has demonstrated enhanced gamma power by reduced NMDA input to fast spiking interneurons, considered to be the target for NMDA antagonists (Spencer, 2009).

In contrast, we found a small but significant decrease in the power of gamma activity recorded in the NAc after injection of ketamine. We found previously that systemic injection of the more selective NMDA antagonist 0.5 mg/kg MK801 robustly reduces the power of gamma (Hunt et al., 2009a). However, in fentanyl anaesthetized rats ketamine can increase the power of gamma in the accumbens (Hakami et al., 2009). Region-specific changes in gamma power have been observed in vitro where ketamine has been shown to increase and decrease gamma power in the auditory and entorhinal cortex, respectively (Cunningham et al., 2006; Roopun et al., 2008). Decreases in gamma power to a conditioned tone have also been found in the PFC and ventral hippocampus of the methylazoxymethanol acetate rat model of schizophrenia, which were associated with reductions in parvalbumin interneuron functionality (Lodge et al., 2009).

Gamma oscillations are involved in many aspects of cognitive function, such as attention and short-term memory. Typically, EEG scalp recordings from schizophrenia patients show a reduction in the power of gamma oscillations (Herrmann and Demiralp, 2005). However, a few studies have found the power of gamma oscillations to correlate positively with a number of the symptoms (Light et al., 2006; Spencer et al., 2004) and a recent human study has also found an increase in EEG gamma power after ketamine administration (Hong et al., 2010). As suggested by others, opposing effects on gamma power may profoundly influence functional connectivity across brain regions and as such fail to support strong synchronization and lead to changes in network dynamics (Roopun et al., 2008). Both the hippocampus and the NAc have been implicated in the pathophysiology of psychiatric diseases, like schizophrenia (O'Donnell and Grace, 1998), and opposing changes in gamma power may represent oneway ketamine leads to disruption of normal information processing.

Acknowledgements

This work was funded by a statutory grant awarded by the Nencki Institute of Experimental Biology and grant NN303345435 from the Polish Ministry of Science and Higher Education. MJH received additional support from the Foundation for Polish Science (START-2008). The authors wish to thank Maciej Olszewski for technical assistance. SŁ was funded by grant PBZ/MNiSW/07/2006/11 from the Polish Ministry of Science and Higher Education.

References

Berke JD (2006) Participation of striatal neurons in large-scale oscillatory networks. In: Bolam JP, Ingham CA, Magill PJ (eds) *The Basal Ganglia VIII*. New York: Springer, 25–35.

Berke JD, Okatan M, Skurski J, Eichenbaum HB (2004) Oscillatory entrainment of striatal neurons in freely moving rats. *Neuron* 43: 883–896.

Boyer P, Phillips JL, Rousseau FL, Ilivitsky S (2007) Hippocampal abnormalities and memory deficits: new evidence of a strong pathophysiological link in schizophrenia. *Brain Res Rev* 54: 92–112.

Brovelli A, Ding M, Ledberg A, Chen Y, Nakamura R, Bressler SL (2004) Beta oscillations in a large-scale sensorimotor cortical network: directional influences revealed by Granger causality. *Proc Natl Acad Sci USA* 101: 9849–9854.

Brown P, Oliviero A, Mazzone P, Insola A, Tonali P, Di Lazzaro V (2001) Dopamine dependency of oscillations between subthalamic nucleus and pallidum in Parkinson's disease. *J Neurosci* 21: 1033–1038.

Buzsaki G (1986) Hippocampal sharp waves: their origin and significance. *Brain Res* 398: 242–252.

Buzsaki G, Chen LS, Gage FH (1990) Spatial organization of physiological activity in the hippocampal region: relevance to memory formation. *Prog Brain Res* 83: 257–268.

Buzsaki G, Leung LW, Vanderwolf CH (1983) Cellular bases of hippocampal EEG in the behaving rat. *Brain Res* 287: 139–171.

Canolty RT, Edwards E, Dalal SS, et al. (2006) High gamma power is phase-locked to theta oscillations in human neocortex. *Science* 313: 1626–1628.

Chrobak JJ, Buzsaki G (1996) High-frequency oscillations in the output networks of the hippocampal-entorhinal axis of the freely behaving rat. *J Neurosci* 16: 3056–3066.

Chrobak JJ, Lorincz A, Buzsaki G (2000) Physiological patterns in the hippocampo-entorhinal cortex system. *Hippocampus* 10: 457–465.

Cohen MX, Axmacher N, Lenartz D, Elger CE, Sturm V, Schlaepfer TE (2009) Good vibrations: cross-frequency coupling in the human nucleus accumbens during reward processing. *J Cogn Neurosci* 21: 875–889.

Crone NE, Sinai A, Korzeniewska A (2006) High-frequency gamma oscillations and human brain mapping with electrocorticography. *Prog Brain Res* 159: 275–295.

Csicsvari J, Hirase H, Czurko A, Buzsaki G (1998) Reliability and state dependence of pyramidal cell-interneuron synapses in the hippocampus: an ensemble approach in the behaving rat. *Neuron* 21: 179–189.

Cunningham MO, Hunt J, Middleton S, et al. (2006) Region-specific reduction in entorhinal gamma oscillations and parvalbumin-immunoreactive neurons in animal models of psychiatric illness. *J Neurosci* 26: 2767–2776.

Darbin O, Newton L, Wichmann T (2006) A new probe to monitor the effects of drugs on local field potentials. *J Neurosci Methods* 155: 291–295.

DeCoteau WE, Thorn C, Gibson DJ, et al. (2007) Oscillations of local field potentials in the rat dorsal striatum during spontaneous and instructed behaviors. *J Neurophysiol* 97: 3800–3805.

Draguhn A, Traub RD, Bibbig A, Schmitz D (2000) Ripple (approximately 200-Hz) oscillations in temporal structures. *J Clin Neurophysiol* 17: 361–376.

Enomoto T, Floresco SB (2009) Disruptions in spatial working memory, but not short-term memory, induced by repeated ketamine exposure. *Prog Neuropsychopharmacol Biol Psychiatry* 33: 668–675.

Finnerty GT, Jefferys JG (2000) 9–16 Hz oscillation precedes secondary generalization of seizures in the rat tetanus toxin model of epilepsy. *J Neurophysiol* 83: 2217–2226.

Fogelson N, Williams D, Tijssen M, van BG, Speelman H, Brown P (2006) Different functional loops between cerebral cortex and the subthalmic area in Parkinson's disease. *Cereb Cortex* 16: 64–75.

Freedman R, Goldowitz D (2009) Studies on the hippocampal formation: from basic development to clinical applications: studies on schizophrenia. *Prog Neurobiol*. doi:10.1016/j.pneurobio.2009.10.008.

Girardeau G, Benchenane K, Wiener SI, Buzsaki G, Zugaro MB (2009) Selective suppression of hippocampal ripples impairs spatial memory. *Nat Neurosci* 12: 1222–1223.

Glasgow SD, Chapman CA (2007) Local generation of theta-frequency EEG activity in the parasubiculum. *J Neurophysiol* 97: 3868–3879.

Grace AA (2000) Gating of information flow within the limbic system and the pathophysiology of schizophrenia. *Brain Res Brain Res Rev* 31: 330–341.

Gruber AJ, O'Donnell P (2009) Bursting activation of prefrontal cortex drives sustained up states in nucleus accumbens spiny neurons in vivo. *Synapse* 63: 173–180.

Hakami T, Jones NC, Tolmacheva EA, et al. (2009) NMDA receptor hypofunction leads to generalized and persistent aberrant gamma oscillations independent of hyperlocomotion and the state of consciousness. *PLoS One* 4: e6755.

Herrmann CS, Demiralp T (2005) Human EEG gamma oscillations in neuropsychiatric disorders. *Clin Neurophysiol* 116: 2719–2733.

Homayoun H, Moghaddam B (2007) Fine-tuning of awake prefrontal cortex neurons by clozapine: comparison with haloperidol and N-desmethylclozapine. *Biol Psychiatry* 61: 679–687.

Hong LE, Summerfelt A, Buchanan RW, et al. (2010) Gamma and delta neural oscillations and association with clinical symptoms under subanesthetic ketamine. *Neuropsychopharmacology* 35(3): 632–640.

Hunt MJ, Falinska M, Kasicki S (2010) Local injection of MK801 modifies oscillatory activity in the nucleus accumbens in awake rats. *J Psychopharmacol* 24: 931–941.

Hunt MJ, Garcia R, Large CH, Kasicki S (2008) Modulation of high-frequency oscillations associated with NMDA receptor hypofunction in the rodent nucleus accumbens by lamotrigine. *Prog Neuropsychopharmacol Biol Psychiatry* 32: 1312–1319.

Hunt MJ, Kessal K, Garcia R (2005) Ketamine induces dopamine-dependent depression of evoked hippocampal activity in the nucleus accumbens in freely moving rats. *J Neurosci* 25: 524–531.

Hunt MJ, Matulewicz P, Gottesmann C, Kasicki S (2009b) State-dependent changes in high-frequency oscillations recorded in the rat nucleus accumbens. *Neuroscience* 164: 380–386.

Hunt MJ, Raynaud B, Garcia R (2006) Ketamine dose-dependently induces high-frequency oscillations in the nucleus accumbens in freely moving rats. *Biol Psychiatry* 60: 1206–1214.

Jackson ME, Homayoun H, Moghaddam B (2004) NMDA receptor hypofunction produces concomitant firing rate potentiation and burst activity reduction in the prefrontal cortex. *Proc Natl Acad Sci USA* 101: 8467–8472.

Jones MS, Barth DS (1999) Spatiotemporal organization of fast (>200 Hz) electrical oscillations in rat Vibrissa/Barrel cortex. *J Neurophysiol* 82: 1599–1609.

Kelley AE, Domesick VB (1982) The distribution of the projection from the hippocampal formation to the nucleus accumbens in the rat: an anterograde- and retrograde-horseradish peroxidase study. *Neuroscience* 7: 2321–2335.

Krystal JH, Karper LP, Seibyl JP, et al. (1994) Subanesthetic effects of the noncompetitive NMDA antagonist, ketamine, in humans. Psychotomimetic, perceptual, cognitive, and neuroendocrine responses. *Arch Gen Psychiatry* 51: 199–214.

Lahti AC, Koffel B, LaPorte D, Tamminga CA (1995) Subanesthetic doses of ketamine stimulate psychosis in schizophrenia. *Neuropsychopharmacology* 13: 9–19.

Large CH, Webster EL, Goff DC (2005) The potential role of lamotrigine in schizophrenia. *Psychopharmacology (Berl)* 181: 415–436.

Leski S, Wojcik DK, Tereszczuk J, Swiejkowski DA, Kublik E, Wrobel A (2007) Inverse current-source density method in 3D: reconstruction fidelity, boundary effects, and influence of distant sources. *Neuroinformatics* 5: 207–222.

Light GA, Hsu JL, Hsieh MH, et al. (2006) Gamma band oscillations reveal neural network cortical coherence dysfunction in schizophrenia patients. *Biol Psychiatry* 60: 1231–1240.

Lodge DJ, Behrens MM, Grace AA (2009) A loss of parvalbumin-containing interneurons is associated with diminished oscillatory activity in an animal model of schizophrenia. *J Neurosci* 29: 2344–2354.

Ma J, Leung LS (2000) Relation between hippocampal gamma waves and behavioral disturbances induced by phencyclidine and methamphetamine. *Behav Brain Res* 111: 1–11.

Ma J, Leung LS (2007) The supramammillo-septal-hippocampal pathway mediates sensorimotor gating impairment and hyperlocomotion induced by MK-801 and ketamine in rats. *Psychopharmacology (Berl)* 191: 961–974.

Magill PJ, Sharott A, Harnack D, Kupsch A, Meissner W, Brown P (2005) Coherent spike-wave oscillations in the cortex and subthalamic nucleus of the freely moving rat. *Neuroscience* 132: 659–664.

Masimore B, Kakalios J, Redish AD (2004) Measuring fundamental frequencies in local field potentials. *J Neurosci Methods* 138: 97–105.

Moghaddam B, Adams B, Verma A, Daly D (1997) Activation of glutamatergic neurotransmission by ketamine: a novel step in the pathway from NMDA receptor blockade to dopaminergic and cognitive disruptions associated with the prefrontal cortex. *J Neurosci* 17: 2921–2927.

Nunez PL, Srinivasan, R (2005) *Electric Fields of the Brain: The Neurophysics of EEG*. Oxford: Oxford University Press.

O'Donnell P, Grace AA (1995) Synaptic interactions among excitatory afferents to nucleus accumbens neurons: hippocampal gating of prefrontal cortical input. *J Neurosci* 15: 3622–3639.

O'Donnell P, Grace AA (1998) Phencyclidine interferes with the hippocampal gating of nucleus accumbens neuronal activity in vivo. *Neuroscience* 87: 823–830.

Paxinos W, Watson C (1986) *The Rat Brain in Stereotaxic Coordinates*. London: Academic Press.

Pennartz CM, Lee E, Verheul J, Lipa P, Barnes CA, McNaughton BL (2004) The ventral striatum in off-line processing: ensemble reactivation during sleep and modulation by hippocampal ripples. *J Neurosci* 24: 6446–6456.

Pettersen KH, Devor A, Ulbert I, Dale AM, Einevoll GT (2006) Current-source density estimation based on inversion of electrostatic forward solution: effects of finite extent of neuronal activity and conductivity discontinuities. *J Neurosci Methods* 154: 116–133.

Pinault D (2008) N-methyl d-aspartate receptor antagonists ketamine and MK-801 induce wake-related aberrant gamma oscillations in the rat neocortex. *Biol Psychiatry* 63: 730–735.

Ponomarenko AA, Korotkova TM, Haas HL (2003) High-frequency (200 Hz) oscillations and firing patterns in the basolateral amygdala and dorsal endopiriform nucleus of the behaving rat. *Behav Brain Res* 141: 123–129.

Rajagovindan R, Ding M (2008) Decomposing neural synchrony: toward an explanation for near-zero phase-lag in cortical oscillatory networks. *PLoS One* 3: e3649.

Roopun AK, Cunningham MO, Racca C, Alter K, Traub RD, Whittington MA (2008) Region-specific changes in gamma and beta2 rhythms in NMDA receptor dysfunction models of schizophrenia. *Schizophr Bull* 34: 962–973.

Sams-Dodd F (1999) Phencyclidine in the social interaction test: an animal model of schizophrenia with face and predictive validity. *Rev Neurosci* 10: 59–90.

Sauleau P, Eusebio A, Thevathasan W, et al. (2009) Involvement of the subthalamic nucleus in engagement with behaviourally relevant stimuli. *Eur J Neurosci* 29: 931–942.

Singer W (1999) Neuronal synchrony: a versatile code for the definition of relations? *Neuron* 24: 49–25.

Spencer KM (2009) The functional consequences of cortical circuit abnormalities on gamma oscillations in schizophrenia: insights from computational modeling. *Front Hum Neurosci* 3: 33.

Spencer KM, Nestor PG, Perlmutter R, et al. (2004) Neural synchrony indexes disordered perception and cognition in schizophrenia. *Proc Natl Acad Sci USA* 101: 17288–17293.

Verma A, Moghaddam B (1996) NMDA receptor antagonists impair prefrontal cortex function as assessed via spatial delayed alternation performance in rats: modulation by dopamine. *J Neurosci* 16: 373–379.

Wilson CJ (1993) The generation of natural firing patterns in neostriatal neurons. *Prog Brain Res* 99: 277–297.

Wilson CJ, Kawaguchi Y (1996) The origins of two-state spontaneous membrane potential fluctuations of neostriatal spiny neurons. *J Neurosci* 16: 2397–2410.

Wojcik DK, Leski S (2010) Current source density reconstruction from incomplete data. *Neural Comput* 22: 48–60.

Ylinen A, Bragin A, Nadasdy Z, et al. (1995) Sharp wave-associated high-frequency oscillation (200 Hz) in the intact hippocampus: network and intracellular mechanisms. *J Neurosci* 15: 30–46.